



Badshah, I.I., Brown, S., Weibel, L., Rose, A., Way, B., Sebire, N., Inman, G., Harper, J. and O'Shaughnessy, R.F.L. (2019) Differential expression of secreted factors SOSTDC1 and ADAMTS8 cause profibrotic changes in linear morphoea fibroblasts. *British Journal of Dermatology*, 180(5), pp. 1135-1149. (doi:[10.1111/bjd.17352](https://doi.org/10.1111/bjd.17352)).

This is the author's final accepted version.

There may be differences between this version and the published version. You are advised to consult the publisher's version if you wish to cite from it.

<http://eprints.gla.ac.uk/178633/>

Deposited on: 24 January 2019

Enlighten – Research publications by members of the University of Glasgow

<http://eprints.gla.ac.uk>

DR RYAN O'SHAUGHNESSY (Orcid ID : 0000-0002-3701-0267)

Article type : Original Article

Corresponding author mail id:r.f.l.oshaughnessy@qmul.ac.uk

Differential expression of secreted factors *SOSTDC1* and *ADAMTS8* cause pro-fibrotic changes in linear morphea fibroblasts.

Running title: Linear morphea fibroblasts show consistent gene expression changes

I. I. Badshah^{1,2*}, S. Brown^{1,2,3*}, L. Weibel⁴, A. Rose⁵, B. Way^{1,2}, N. Sebire⁶, G. Inman⁵, J. Harper^{1,2}, V. Kinsler^{1,2}, R. O'Shaughnessy^{1,2,7}

1) Immunobiology and Dermatology, UCL Institute of Child Health, London, UK

2) Livingstone Skin Research Centre, UCL Institute of Child Health, London, UK

3) Restoration of Appearance and Function Trust, Leopold Muller Building, Mount Vernon Hospital, Northwood, Middlesex, UK

4) Department of Dermatology, University Hospital, Zurich, Switzerland

5) Division of Cancer Research, University of Dundee, School of Medicine, Dundee, UK

6) Histopathology, Great Ormond Street Hospital, London, UK

7) Centre for Cell Biology and Cutaneous Research, Blizard Institute, Queen Mary University of London, UK

Corresponding Author: Ryan F.L. O'Shaughnessy, Centre for Cell Biology and Cutaneous Research, Blizard Institute, Queen Mary University of London School of Medicine and Dentistry, 4 Newark Street London, E1 2AT, Phone +44 207 882 2335

* These authors contributed equally

This article has been accepted for publication and undergone full peer review but has not been through the copyediting, typesetting, pagination and proofreading process, which may lead to differences between this version and the Version of Record. Please cite this article as doi: 10.1111/bjd.17352

This article is protected by copyright. All rights reserved.

Funding: RO, IB and SB are funded by the Great Ormond Street Children's Charity. This research was supported by the NIHR Great Ormond Street Hospital Biomedical Research Centre. The views expressed are those of the author(s) and not necessarily those of the NHS, the NIHR or the Department of Health.

There are no conflicts of interest

What's already known about this topic:

- Linear morphoea (LM) is a rare connective tissue disorder
- The underlying mechanism responsible for the fibrosis of LM is unknown.

What does this study add?

- LM fibroblasts from diseased skin possess a persistent, identifiable cell phenotype
- LM fibroblasts display increased cell growth, and migration, and reduced response to TGF- β 1.

What is the translational message:

- Cell-intrinsic changes in the LM fibroblast secretome lead to changes observed in the disease,
- Secretome modulation could be a viable therapeutic approach in the treatment of LM.

Manuscript

ABSTRACT

Background: Linear morphoea (LM) is a rare connective tissue disorder characterised by a line of thickened skin and subcutaneous tissue and can also affect the underlying muscle and bone. Little is known about disease aetiology, with treatment currently limited to immune suppression, and disease recurrence post-treatment is common.

Objective: To uncover new therapeutic avenues, the cell intrinsic changes in LM fibroblasts compared to site-matched controls was characterised.

Methods: We grew fibroblasts from site matched affected and unaffected regions from 5 linear morphoea patients, we subjected them to gene expression analysis and investigation of SMAD signalling.

Results: Fibroblasts from LM lesions showed increased migration, proliferation, altered collagen processing, as well as abnormally high basal levels of phosphorylated SMAD2, thereby rendering them less responsive to TGF- β 1 and reducing the degree of myofibroblast differentiation, a key component of the wound healing and scarring process in normal skin. Conditioned media from normal fibroblasts could reverse LM affected fibroblast migration and proliferation, suggesting that the LM phenotype is driven by an altered secretome. Gene array analysis and RNA-Seq indicated upregulation of *ADAMTS8* and downregulation of *FRAS1* and *SOSTDC1*. *SOSTDC1* knockdown

recapitulated the reduced TGF- β 1 responsiveness and LM fibroblast migration, whilst overexpression of ADAMTS8 induced myofibroblast markers.

Conclusions: We demonstrate that cell-intrinsic changes in the LM fibroblast secretome lead to changes observed in the disease, and that secretome modulation could be a viable therapeutic approach in the treatment of LM.

Abbreviations: LM, linear morphoea; TGF- β , transforming growth factor beta; ECM, extracellular matrix; ADAMTS8, ADAM metalloproteinase with thrombospondin type 1 motif 8; FRAS1, Fraser extracellular matrix complex subunit 1; SOSTDC1, Sclerostin domain containing 1; ALK, activin receptor-like kinase; SMAD, mothers against decapentaplegic homolog; MMP, matrix metalloproteinase; α -SMA, α -smooth muscle actin;

Keywords: Linear morphoea, fibrosis, migration, proliferation, secreted proteins, TGF- β

INTRODUCTION

The fibrotic disorder of linear morphoea (LM) represents the most prevalent subtype of localised scleroderma (morphoea) in children [1]. Morphoea can be classified according to clinical phenotype which include the plaque, generalised, linear, and deep subtypes. LM typically occurs in childhood with its prevalence being greater in the young relative to systemic scleroderma (systemic sclerosis) [2]. Almost entirely restricted to tissues descended from the mesoderm, it possesses a distinct gene signature distinguishable from most systemic scleroderma samples in spite of sharing the principal pathology of dysregulated collagen production and degradation [1,3]. Consequently, the disease displays thickening and hardening of the skin [2]. In addition to the dermis, the underlying subcutaneous tissue, bone and central nervous system are also susceptible [1]. Disease progression begins with an inflammatory phase followed by skin hyperaemia, fibrosis, sclerosis and lastly tissue atrophy [2]. The poor heritability of the disease, with no identified gene defect, suggests that it is a multivariant disorder, with possible risk factors including a family history of autoimmune disease or environment events. The disease also shows an approximate 2.5:1 bias toward females [2]. There is indication that this disease is a consequence of genetic mosaicism as the lesions correlate with the lines of Blaschko [2]. Novel treatment modalities could be informed by the specific gene expression differences between the affected and unaffected regions of the skin.

Fibrosis involves the production of extracellular matrix (ECM) constituents such as collagens during the physiological wound healing process as well as in pathologies of excessive or aberrant scarring. The fibroblast is responsible for the organisation of the ECM and represents a critical component of fibrogenesis. Fibroblasts are activated by mechanical stress to form proto-myofibroblasts, which with the addition of the ED-A splice variant of fibronectin and transforming growth factor- β 1 (TGF- β 1) differentiate into α -smooth muscle actin (α -SMA) expressing myofibroblasts [4]. The myofibroblast is the principal ECM producing cell and their persistence in most fibro-contractile diseases highlights their important regulatory role in resolving fibrotic processes [4].

TGF- β 1 is a significant facilitator of the fibrosis of many tissues and mediates numerous processes that cover differentiation, proliferation, migration, and apoptosis [5]. TGF- β 1 is synthesised as a precursor which is cleaved intracellularly to produce the latency-associated peptide from the N-terminus and the TGF- β 1 homodimer from the C-terminus [6]. Proteolytically activated TGF- β 1 binds and induces phosphorylation in its cognate receptor consisting of the TGF- β type I (T β RI) and TGF- β type II (T β RII) homodimers [7]. Canonical TGF- β 1 signalling is mediated by the specific T β RI activin receptor-like kinase (ALK) 5, which upon activation leads to the recruitment and phosphorylation of the receptor-regulated mothers against decapentaplegic homolog (SMAD) 2 and 3 [7]. The receptor-regulated SMADs then complex with the common-mediator SMAD4 and translocate into the nucleus to control gene expression [5].

The underlying mechanism responsible for the fibrosis of LM is unknown. The aim of this study was to improve understanding of the disease by investigating phenotypic differences between fibroblasts isolated from LM lesions and normal skin regions. Gene expression analysis was performed to identify possible mediators of these distinct disease phenotypes, followed by subsequent over- and underexpression of selected genes to identify potential therapeutic targets. We show that LM fibroblasts from diseased skin possess a persistent, identifiable cell phenotype in culture exhibiting increased cell growth, increased migration, and paradoxically a reduced response to TGF- β 1. Knockdown and overexpression studies demonstrated that dysregulation of the secretome underlies the phenotype of LM fibroblasts.

MATERIALS AND METHODS

Cell culture

Human primary dermal fibroblasts were isolated from punch biopsies of affected (A) areas and site-matched normal (N) regions of consented patients with linear morphea (Table 1) by trypsin/collagenase digestion (Sigma-Aldrich) and were subsequently expanded. Human primary dermal fibroblasts and mouse NIH 3T3 fibroblasts were cultured in DMEM (low glucose; Sigma-Aldrich) supplemented with FBS (10% v/v; ThermoFisher Scientific) and Antibiotic-Antimycotic (1% v/v; ThermoFisher Scientific) in a humidified atmosphere of 5% CO₂ and 95% air at 37°C, with media changes occurring thrice weekly. Cells from passage 3-7 were used in experiments.

Stimuli and inhibitors

Cells were serum-starved overnight and treated in serum-free culture media. Detection of α -SMA-expressing fibroblasts was conducted by 48 h serum-reduction in culture media containing FBS (0.1% v/v). Cells were treated with the growth factor TGF- β 1 (12.5 ng/ml; Sigma-Aldrich) in media additionally containing BSA (0.1% w/v; Sigma-Aldrich), the DNA synthesis inhibitor mitomycin C (10 μ g/ml; Sigma-Aldrich) with a 30 min pre-incubation. Control vehicles were culture media plus BSA (0.1% w/v) in place of TGF- β 1, and dimethyl sulphoxide (DMSO; 0.1% v/v; Sigma-Aldrich) in place of the inhibitors. Conditioned media was generated by serum-starving cells for 24 h followed by 2 rinses in PBS (MP Biomedicals) and incubating cells with serum-free media for 24 h; this was mixed 1:1 with fresh serum-free DMEM before application to replenish depleted nutrients.

Transfection and transduction of fibroblasts

Mouse NIH 3T3 fibroblasts were stably transfected with Lipofectamine 2000 (Invitrogen) with mouse Sostdc1 (NM_025312) SureSilencing shRNA Plasmids (Qiagen), or scrambled sequence negative control plasmids (Qiagen) according to manufacturer's instructions. Cells were selected in fresh complete media containing G 418 (400 µg/ml; Sigma-Aldrich) and were maintained in G 418 (200 µg/ml). Sostdc1 protein levels in conditioned media were assessed following PNGase F (New England Biolabs) treatment for 1 h to remove glycosylations.

Linear morphoea normal primary dermal fibroblasts were stably transduced with: ADAMTS8 (NM_007037) Human LentiORF Particles (pLenti-C-mGFP-P2A-Puro; OriGene) for overexpression, or LentiORF Control Particles (pLenti-C-mGFP-P2A-Puro; OriGene) as an empty vector control. Cells at ~50% confluency were incubated overnight in complete media with polybrene (8 µg/ml; Sigma-Aldrich) at an MOI of 6. Subsequently, the lentivirus-containing media was replaced with fresh complete media for 24 h. Cells were then selected in fresh complete media plus puromycin (2 µg/ml; Sigma-Aldrich) according to a puromycin titration (data not shown) to select for successfully transduced cells. After ~10 days, with selection media being replaced routinely every 3-4 days, puromycin-resistant colonies were expanded and used in experimentation.

BrdU incorporation proliferation assay

Cells were seeded in triplicate into a 96 well microplate at a density of 1×10^3 cells/cm², cultured overnight and BrdU incorporation with visualisation by peroxidase was assayed according to manufacturer's instructions (Millipore). Absorbance (450 nm) was detected with the Multiskan EX spectrophotometer (Thermo Scientific).

Scratch motility assay

Cells were seeded in triplicate into 6 well plates at a density of 5×10^4 cells/cm² and cultured overnight. Confluent cells were pre-incubated for 30 min with mitomycin C (10 µg/ml) to inhibit proliferation, scratched with a 20 µl pipette tip, rinsed twice in serum-free DMEM to remove cell debris, and then incubated in DMEM containing mitomycin C (10 µg/ml) plus additional treatments. Images were taken in triplicate for each condition with the Olympus IX71 inverted microscope and HCLImage Live (v4.3) capture software at 0 h to acquire baseline images, and at the experiment end-point of 24 h. Image analysis was conducted using the Fiji distribution of ImageJ (v1.51n). The denuded area was measured using the 'Polygon Selection' tool. End-point data was normalised to the denuded area at 0 h.

Adhesion assay

Cells were seeded into a 96 well microplate at a density of 1×10^4 cells/cm², cultured overnight, and treatments applied. At the experiment end-point, non-adherent cells were removed by rinsing in PBS and the microplate was then frozen at -70°C for at least 24 h to allow for efficient cell lysis. The

microplate was thawed and incubated for 5 min, protected from light, with a solution of the nucleic acid fluorescent dye CyQUANT GR (1×, excitation: 485 nm, emission 520 nm; ThermoFisher Scientific) and Cell Lysis Buffer (1×; ThermoFisher Scientific) according to the manufacturer's instructions. The sample fluorescence was then measured with the FLUOstar OPTIMA fluorescence plate reader (BMG Labtech).

Collagen gel contraction assay

Into 6 well plates 1×10^5 cells/well were mixed with a solution of Bovine Collagen I (4 mg/ml; Invitrogen) and Hank's Balanced Salt Solution (1×, pH 7.2; Sigma-Aldrich), seeded and allowed to set at 37°C in a stainless steel washer (135 mm), which was subsequently removed. Baseline 0 h images and day 8 end-point images were acquired using the Leica DFC320 microscope (Leica Microsystems). Gel contraction was measured as gel area at day 8 normalised to the initial gel area of 0 h images using the Fiji distribution of ImageJ.

TGF-β1 ELISA

Secreted TGF-β1 in 24 h conditioned media was determined using the Human/Mouse TGF beta1 ELISA Ready-SET-Go! (2nd Generation; eBioscience) according to manufacturer's instructions. Absorbance (450 nm) was detected with the Multiskan EX spectrophotometer.

Immunofluorescence

Paraffin-embedded tissue sections (5 μm) were prepared with standard protocols. To study immunofluorescence *in vitro*, cells on coverslips were fixed and permeabilised for 10 min in a warm solution of PFA (4% v/v) and Triton X-100 (0.1% v/v; Sigma-Aldrich), followed by a 5 min wash in PBS. Tissue sections and *in vitro* samples were blocked for 30 min or 1 h, respectively, in Fish Skin Gelatin (0.8 % v/v; Sigma-Aldrich) plus Triton X-100 (0.2 % v/v). Primary antibodies (SOSTDC1, 1:500, Abcam; ACTA2, 1:500, Dako; p-SMAD2, 1:250, Cell Signaling Technology; p-SMAD2,3, 1:250, Cell Signaling Technology; ADAMTS8 2H5, 1:100, Novus Biologicals; FRAS1 H-300, 1:200, Santa Cruz Biotechnology) diluted in blocking buffer were incubated at 4°C overnight. Sections and cells were washed in PBS-Tween 20 (PBS-T, 0.1% v/v; Sigma-Aldrich) and then incubated at room temperature for up to 1 h with Alexa Fluor-conjugated secondary antibodies (1:500; Invitrogen) diluted in blocking buffer. Sections and cells were mounted in ProLong Gold Antifade Mountant with DAPI (Invitrogen). Images were acquired with Micro-Manager (v1.4.21) software and analysis was performed with the Fiji distribution of ImageJ. Picosirius red histology was imaged using an epifluorescence microscope with side illumination.

Western blotting

Protein lysates were harvested on ice by scraping and vortexing with lysis buffer [Tris-HCl (20 mM), pH 7.5, NaCl (150 mM), EDTA (1 mM), Triton X-100 (1% v/v), sodium deoxycholate (0.5% w/v), SDS (0.1% w/v), protease inhibitor cocktail (1×; Roche), phosphatase inhibitor cocktail (2×; Roche)]. Protein concentration was quantified with the Bradford Protein Assay (Bio-Rad). Equal amounts were electrophoresed in Mini-PROTEAN TGX Precast Protein Gels (4-20%; Bio-Rad) in Tris-Glycine-SDS buffer [1×, Tris base (0.25 M), glycine (1.92 M), SDS (1% w/v); Scientific Laboratory Supplies]. Proteins were transferred onto Amersham Protran Nitrocellulose Blotting Membranes (0.45 μm; GE Life Sciences) with Pierce Western Blot Transfer Buffer (ThermoFisher Scientific). Membranes were blocked for 30 min in dried skimmed milk (5% w/v; Marvel) in PBS-T and incubated at 4°C overnight with primary antibodies (p-SMAD2, 1:250, Abcam; SMAD2, 1:500, Cell Signaling Technology; p-SMAD3, 1:250, Cell Signaling Technology; SMAD3, 1:250, Cell Signaling Technology; MMP-2, 1:250; Alpha Smooth Muscle Actin, 1:250, Abcam; ADAMTS8 2H5, 1:500, Novus Biologicals; FRAS1 H-300, 1:200, Santa Cruz Biotechnology; GAPDH, 1:2000, Merck-Millipore). Subsequently, membranes were subjected to 5 min washes in PBS-T and then incubated with HRP-conjugated secondary antibodies (1:3000; Dako). Membranes were visualised with the Amersham ECL Prime detection kit (GE Life Sciences) and Hyperfilm ECL (GE Life Sciences). Densitometry was performed with the Fiji distribution of ImageJ.

Gelatin zymography

Equal volumes of 24 h conditioned media aspirated from 1×10^6 cells for each condition were separated by non-denaturing electrophoresis in a gelatin (0.5% w/v) acrylamide-*bis*-acrylamide gel (7.5% w/v), and then incubated for 24 h at 35°C in enzymatic reaction buffer [Tris-HCl (0.05 M), pH 7.4, NaCl (20 mM), CaCl₂ (5 mM), NaN₃ (0.02% w/v)] to allow digestion of gelatin. The gel was stained with Coomassie Brilliant Blue R-250 Dye (ThermoFisher Scientific) at room temperature for ~10 min to detect undigested regions and was subsequently destained with a solution of methanol (30% v/v) and acetic acid (10% v/v). MMP bands were discerned by protein size with reference to a protein ladder. Conditioned media run in gels lacking gelatin and stained with Coomassie Brilliant Blue R-250 Dye was used as a loading control.

Microarray analysis and RNA sequencing

Total RNA was extracted from low passage number cells and DNase treated with the RNeasy kit according to manufacturer's instructions (Qiagen). RNA quality was assessed with a Nanodrop 2000c spectrophotometer (Thermo Scientific) and an Agilent Bioanalyser 2100 (Agilent Technologies). Total RNA (~2 μg) from each sample was used to generate double-stranded cDNA using a T7-oligo (dT) primer. Biotinylated cRNA, produced by *in vitro* transcription, was fragmented and hybridised to an Affymetrix Human Genome U133 Plus 2.0 microarray (48,000 probesets; ThermoFisher Scientific). The arrays were processed with a GeneChip Fluidics Station 450 (ThermoFisher Scientific) and scanned on an Affymetrix GeneChip Scanner (ThermoFisher Scientific), according to standard protocols. Expression signals were normalised to remove background noise and non-biological

variations amongst arrays. Background noise was removed from the PM probe intensities using the “RMA” method. Primary data was calculated using both Microarray Analysis Suite (v5.0; Affymetrix) including mismatch probeset controls and GC-RM (quantile normalised).

RNA-Seq was performed by UCL Genomics with libraries being synthesised from total RNA (2 µg) with an RNA integrity value of > 8 in all cases; libraries were sequenced with a 36 bp paired end read. The generated FastQ files were mapped against the *Homo sapiens* reference sequence GRCh37/hg19 using Bowtie, TopHat and SAMtools; duplicate reads were removed with SAMtools and read counts per gene were generated using HTSeq-count. EdgeR (Bioconductor) was used to normalise gene expression and generate lists of differentially expressed genes (DEGs). DEGs altered at least 2-fold in expression with *P* value < 0.05 in ≥ 4 of 5 sample pairs. This trimmed data set was then analysed by DAVID for gene ontology (GO) term enrichment with Bonferroni correction for multiple testing.

RESULTS

LM fibroblasts are hyperproliferative, hypermigratory, with altered collagen processing

Tissue harvested from LM patients of affected lesions and site-matched normal skin was stained with haematoxylin and eosin. There were clumps of vimentin positive fibroblasts in the reticular dermis distal from the epidermis in affected dermis, but overall numbers of fibroblasts were unchanged. Collagen arrangement was altered in the dermis according to picosirius red staining (Figure 1A). Differences between LM fibroblasts from normal and affected areas were investigated using primary human dermal fibroblasts isolated and cultured *in vitro* (Table 1). Given the relative increased presence of fibroblasts in affected regions, proliferation was studied by performing cell counts on fibroblasts initially seeded at equal densities and cultured for 3, 6, 8 and 10 days. At day 10, affected fibroblasts exhibited a greater cell number relative to normal fibroblasts cultured for 10 days (Figure 1B). BrdU incorporation into proliferating cells was increased relative to normal fibroblasts (Figure 1C).

Fibroblast motility was investigated with a scratch assay. The denuded area at 24 h post-scratch with affected fibroblasts was reduced compared to normal fibroblasts indicating increased relative migration (Figure 1D). Activated fibroblasts involved in scar formation during wound healing and fibrotic pathologies exhibit an increase in the capacity to contract collagen gels [8,9]. However, affected fibroblasts demonstrated a diminished capacity to contract collagen gels relative to normal fibroblasts (Figure 1E). TGF-β1 is integral to the development of differentiated myofibroblasts and, consequently, is critically implicated in fibrosis [10,11]. Conditioned media supernatant harvested after 24 h incubation with normal and affected LM fibroblasts did not contain differing levels of secreted TGF-β1 as detected by ELISA (Figure 1F).

Matrix metalloproteinases (MMPs) such as MMP-2 are increased in expression and activity in activated fibroblasts [12]. Western blot analysis of conditioned media from affected fibroblasts displayed modestly (1.3X) increased levels of MMP-2 protein relative to normal fibroblasts (Figure 1G). Additionally, affected fibroblasts demonstrated significantly greater MMP-2 activity relative to normal fibroblasts when conditioned media was subjected to gelatin zymography (Figure 1G and H).

Taken together, LM fibroblasts are hyperproliferative, hypermigratory and have higher levels of collagen processing than fibroblasts at site-matched normal regions of the same individual.

Altered response to TGF- β 1 on the proliferation and adhesion of LM fibroblasts

TGF- β 1 mediates various cellular processes of fibroblasts [13]. To assess the potential modulation of LM fibroblast phenotype, cells were treated with TGF- β 1 (12.5 ng/ml) for 24 h and proliferation was assayed by BrdU incorporation. Although BrdU levels in affected fibroblasts were elevated in comparison to normal fibroblasts, this relative increase was attenuated by TGF- β 1 treatment (Figure 2A).

To explore the effect of secreted factors on LM fibroblast motility, cells were incubated with culture media conditioned for 24 h with the opposite fibroblast type (i.e. normal on affected cells or affected on normal cells) following a scratch in the presence of mitomycin C (10 μ g/ml). The increased motility of affected fibroblasts relative to normal fibroblasts was reduced when the culture media was replaced with that conditioned by normal fibroblasts (Figure 2B). Conditioned medium from affected fibroblasts had no effect on motility of normal fibroblasts (Figure 2B). The influence of a fibrotic environment on the adhesion ability of LM fibroblasts was investigated by incubating cells for 24 h with either TGF- β 1 (12.5 ng/ml) or media conditioned for 24 h with the opposite fibroblast type. Non-adherent cells were removed by rinsing in PBS and remaining cells were assessed by incubation with the nucleic acid fluorescent dye CyQUANT GR. The adhesion of affected fibroblasts was significantly lower than of normal fibroblasts (Figure 2C). TGF- β 1 treatment decreased normal fibroblast adhesion without altering the reduced adhesion of affected fibroblasts further (Figure 2C). Conditioned media incubation greatly decreased normal fibroblast adhesion and consequently demolished the difference relative to affected fibroblasts (Figure 2C). Therefore, proliferation and adhesion along with the resulting response to TGF- β 1 treatment are altered in affected fibroblasts.

The differentiated myofibroblast, whose persistence is central to the fibrotic lesions of many disorders, is typified by the expression of α -SMA [10]. LM lesion-associated fibroblasts demonstrated increased α -SMA relative to normal fibroblasts (Figure 2E). TGF- β 1 (12.5 ng/ml) treatment for 24 h increased α -SMA protein in normal fibroblasts, whereas this was limited in affected fibroblasts (Figure 2E). Affected fibroblasts also displayed less α -SMA immunofluorescence staining 24 h post-scratch wounding relative to normal fibroblasts (Figure 2F).

TGF- β 1 signalling can occur through distinct pathways that involve SMAD2/3 [14]. Affected LM fibroblasts displayed a reduced level of SMAD2 immunofluorescence staining 30 min post-scratch wounding relative to normal cells (Figure 2D). To better understand this differential response of LM fibroblasts following TGF- β 1 stimulation, downstream SMAD signalling was investigated. In unstimulated conditions affected fibroblasts possessed an elevated level of p-SMAD2 protein detected by western blotting relative to normal cells, whereas p-SMAD3 protein levels did not differ (Figure 2G). The application of TGF- β 1 (12.5 ng/ml) for 30 and 60 min did not significantly increase p-SMAD3 levels relative to untreated normal cells (Figure 2G). Increased levels of p-SMAD2 in affected fibroblasts were not elevated further with TGF- β 1 stimulation (Figure 2G).

LM lesions lack SMAD2 phosphorylation compared to scleroderma

Following the discovery of variance in p-SMAD2 and 3 levels between LM fibroblasts harvested from normal and affected regions, differences in LM and scleroderma skin tissue was additionally investigated. Immunohistochemistry revealed widespread nuclear p-SMAD3 staining in the dermis of LM and scleroderma skin, both in the dermis and epidermis (Figure 3A). However, the presence of increased nuclear p-SMAD2 was significantly more frequent in dermis of scleroderma skin compared to LM or normal skin (Figure 3B). Therefore, the reduced nuclear p-SMAD2 expression seen in LM may be diagnostic of the disease.

Gene expression analysis indicates consistent changes in the LM fibroblast secretome

To characterise the differences inherent in LM fibroblasts of affected lesions and normal skin, gene expression analysis was performed. Microarray gene expression analysis (normal 1, 2, 3, and affected 1, 2, 3) was combined with RNA-Seq data (normal 4, 5, and affected 4, 5) which identified 39 significantly differentially expressed genes by at least 2-fold that were common to ≥ 4 of the 5 normal/affected pairs (Figure 4A). Organ development, morphogenesis, tissue development, and extracellular proteins were the only over-represented gene ontology (GO) groups determined by DAVID GO term enrichment (Figure 4B). Of the 39 differentially expressed genes, 9 were secreted proteins (Figure 4C). As the secretome of normal cells could rescue the disease-associated phenotype of LM lesion affected fibroblasts, the subset of differentially expressed genes encoding secreted factors was further examined for fibrosis-centric proteins such as those known to modulate TGF- β 1 signalling or the extracellular matrix (Figure 4C). From this subset Sclerostin domain containing 1 (*SOSTDC1*), ADAM metallopeptidase with thrombospondin type 1 motif 8 (*ADAMTS8*), and Fraser extracellular matrix complex subunit 1 (*FRAS1*) were chosen for further study (Table 2, Figure 4D).

Sostdc1 knockdown increases migration and reduces proliferation and TGF β 1 response

SOSTDC1 is a secreted antagonist of TGF- β superfamily members and a modulator of Wnt signalling, both pathways that promote fibrosis [15–17]. Immunofluorescence staining of *SOSTDC1* in LM skin tissue revealed a reduced signal in fibroblasts of affected regions relative to normal fibroblasts (Figure 5A). Additionally, *SOSTDC1* protein expression was reduced in both the lysate and conditioned media supernatant of affected fibroblasts *in vitro* relative to normal cells (Figure 5B). *SOSTDC1* was secreted in glycosylated form, and PNGaseF treatment was necessary to resolve secreted *SOSTDC1* expression in conditioned medium.

To study the effect of *SOSTDC1* downregulation in LM fibroblasts, mouse NIH 3T3 fibroblasts were transfected with either a scrambled sequence shRNA control or *Sostdc1* shRNA. Conditioned media supernatant harvested from *Sostdc1* shRNA transfected NIH 3T3 cells possessed reduced levels of *Sostdc1* protein relative to scrambled shRNA transfected cells (Figure 5C). *Sostdc1* shRNA transfected fibroblasts exhibited a relative reduction in cell number after 10 days of *in vitro* culture compared to scrambled shRNA transfected cells (Figure 5D). Fibroblasts transfected with *Sostdc1*

shRNA also demonstrated an increase in migration relative to the scrambled shRNA control (Figure 5E). MMP2 levels and activity were unchanged in *Sostdc1* knockdown fibroblasts (Figure 5F).

The influence of *Sostdc1* knockdown on TGF- β 1 downstream signalling was investigated by treating scrambled or *Sostdc1* shRNA transfected NIH 3T3 fibroblasts with or without TGF- β 1 (12.5 ng/ml) for 3 or 6 h. Scrambled shRNA expressing controls exhibited increased p-SMAD2 protein in response to TGF- β 1, whereas in *Sostdc1* shRNA transfected cells following TGF- β 1 stimulation SMAD2 phosphorylation was limited (Figure 5G).

To investigate the result of *Sostdc1* downregulation on fibroblast phenotype, NIH 3T3 cells were transfected with either scrambled or *Sostdc1* shRNA, and treated with or without TGF- β 1 (12.5 ng/ml) with an increasing duration of serum starvation (0, 2 or 24 h). In normal culture conditions *Sostdc1* shRNA expressing fibroblasts possessed elevated levels of α -SMA relative to the respective scrambled shRNA control (Figure 5H). TGF- β 1 treatment of scrambled shRNA fibroblasts increased α -SMA levels relative to untreated scrambled shRNA cells, whereas TGF- β 1 treatment of *Sostdc1* shRNA fibroblasts reduced α -SMA relative to untreated *Sostdc1* shRNA cells (Figure 5H).

FRAS1 protein expression is lost in LM fibroblasts and in the dermis of LM affected skin

FRAS1 is an ECM protein that mediates epidermal-dermal adhesion and is capable of activating TGF- β family members [18–20]. FRAS1 protein was decreased in LM affected fibroblasts relative to normal cells, thereby reflecting the gene expression analysis results (Figure 6A).

Immunofluorescence staining of FRAS1 in LM skin tissue *ex vivo* was reduced in dermal fibroblasts associated with LM lesions compared to normal sites. Furthermore, widespread staining of FRAS1 was seen in the dermis not localised to fibroblasts, whilst epidermal FRAS1 levels did not significantly change (Figure 6B). This suggests that secretion of FRAS1 into the dermis is significantly decreased in LM.

Overexpression of ADAMTS8 induces smooth muscle actin expression in normal fibroblasts

ADAMTS8 is a member of the ADAMTS family of secreted metalloproteases which are implicated in a diverse array of functions including migration, adhesion, proliferation and growth factor signalling [21,22]. ADAMTS8 protein levels were increased in affected fibroblasts associated with LM lesions relative to fibroblasts harvested from normal sites (Figure 6C). Similarly, ADAMTS8 immunofluorescence staining was increased in LM affected fibroblasts relative to normal fibroblasts (Figure 6D).

To study the effect of ADAMTS8 expression on fibroblast phenotype, LM fibroblasts from normal regions were transduced with either an empty vector control or an ADAMTS8 overexpression vector. Fibroblasts overexpressing ADAMTS8 demonstrated an increase in ADAMTS8 protein relative to the empty vector control (Figure 6E). Protein levels of α -SMA were elevated following ADAMTS8 overexpression relative to the empty vector control and thereby emulated the increase observed in affected cells relative to normal fibroblasts (Figure 6E).

DISCUSSION

LM is a mosaic disease where cells present in normal skin and lesions possess a heterogeneous phenotype which is responsible for their separate histology and, consequently, pathology [2]. We show that LM affected fibroblasts possessed a distinct cell-intrinsic phenotype which is responsible for many aspects of disease pathology: increased proliferation, migration, MMP-2 activity, and decreased adhesion. These processes are integral to normal fibroblast function during wound healing and scar formation [23,24]; some of which are additionally involved in scleroderma [25,26]. Constitutive SMAD2 phosphorylation and subsequent insensitivity to TGF- β 1 also contributed to the LM phenotype. Conditioned media swap experiments confirmed that the disease phenotype is driven by secreted proteins. Furthermore, a discrete set of differentially expressed genes, including downregulated *SOSTDC1* and upregulated *ADAMTS8*, promoted different facets of the LM phenotype. It is important to consider when interpreting these experiments that there may be systemic effects caused by methotrexate treatment, although these should be controlled for by site matching in the same patient, or that there may be underlying genetics that predispose to LM. Both could change the biology of the fibroblasts even in the unaffected sites

The finding herein of unaltered levels of TGF- β 1 secretion between normal and affected fibroblasts agrees with studies investigating TGF- β 1 in skin and blood of various forms of scleroderma [13,27]. Although no difference in TGF- β 1 secretion existed between normal and affected fibroblasts, there was instead a distinct response to TGF- β 1 in LM fibroblasts. The reduction in affected fibroblast proliferation with TGF- β 1 stimulation indicates a transition to the myofibroblast phenotype, where differentiation leads to a contractile phenotype whilst proliferation ceases [4]. This altered TGF- β 1 responsiveness could be attributed to LM fibroblasts being skewed towards a myofibroblast phenotype, consistent with the increased α -SMA expression in resting affected fibroblasts, however there may be a stall in the differentiation to a full myofibroblast phenotype as contraction of collagen gels was impaired. It is possible that incomplete myofibroblast differentiation is contributing to the fibrotic phenotype in LM

Canonical TGF- β 1 signalling occurs through the phosphorylation and activation of SMAD2 and SMAD3 [5]. LM tissue displayed a distinct profile of SMAD phosphorylation exhibiting lower p-SMAD2 relative to scleroderma, whereas p-SMAD3 was similar between them. Localised scleroderma fibroblasts exhibit constitutive DNA-SMAD3 binding which was reflected herein [28]. In LM affected fibroblasts it was only SMAD2 that portrayed elevated phosphorylation in the resting state. The implication of this constitutive activation is seen in the elevated α -SMA and consequent myofibroblast phenotype. In human lung fibroblasts, unlike SMAD3, SMAD2 overexpression results in a TGF- β 1-independent alteration of phenotype with an increase in α -SMA [29]. This reinforces SMAD2, not SMAD3 as a crucial mediator in the control of LM fibroblast phenotype. When affected fibroblasts were stimulated into action by either scratch wounding or TGF- β 1 treatment, levels of SMAD2 were lower relative to normal cells and this was also reflected in the reduced α -SMA. This suggests a defect in the ability of affected fibroblasts to respond to such stimuli. A further reason aside from a general dysregulation of SMAD signalling may be that myofibroblasts in dense cultures, such as those arising from the increased proliferation witnessed in affected LM fibroblasts, decrease α -SMA expression and de-differentiate into α -SMA-negative fibroblasts due to contact-induced desensitisation to TGF- β 1 [30].

SOSTDC1 is an inhibitor of bone morphogenetic proteins (BMPs), which belong to the TGF- β superfamily, that prevents cognate receptor association by directly binding to BMPs [16,17]. SOSTDC1 is further indirectly related with TGF- β signalling through its interaction with the Wnt pathway which is activated in many fibrotic diseases [15,31,32]. Therefore, the decreased SOSTDC1 expression and secretion in LM represents a mechanism for the fibrosis, as inhibition of Wnt and SMAD signalling is lost. *Sostdc1* knockdown caused a relative decrease in proliferation contrary to the elevated proliferation of LM affected fibroblasts. It is possible that the resulting disinhibition of TGF- β signalling promotes the fully differentiated, pro-contraction and anti-proliferation myofibroblast phenotype [4]. However, the *Sostdc1* shRNA was sufficient to induce the migratory phenotype of affected LM fibroblasts. This is consistent with the concept that LM fibroblasts are migratory, activated myofibroblast-like cells.

The diminished p-SMAD2 response and limited α -SMA induction with TGF- β 1 treatment of *Sostdc1* transfected fibroblasts mirrored the lack of responsiveness seen in affected LM fibroblasts. Therefore, reduced SOSTDC1 is likely a driver of TGF- β 1 insensitivity in LM fibroblasts. As SOSTDC1 can affect both the TGF- β and Wnt signalling pathways, it is attractive to suggest that loss of SOSTDC1 or related genes can perturb myofibroblast differentiation to induce a pro-fibrotic dermal environment. *Sostdc1* shRNA transfection reproduced the increase in MMP-2 activity and consequent fibroblast migration. However, transfection alone was insufficient to replicate the increase in MMP-2 protein secretion. Since MMP-2 can activate TGF- β 1, this suggests that affected fibroblasts could experience a greater TGF- β 1 response and SMAD2 phosphorylation without a change in TGF- β 1 levels [12].

LM tissue and affected fibroblasts possessed a relative decrease in *FRAS1* gene expression that was replicated at the protein level both *in vitro* and in LM skin tissue *ex vivo*. Mutations in *FRAS1* are responsible for Fraser syndrome which is a severe multisystem condition that occurs during development *in utero* where 45% of individuals are stillborn or die within a year, whilst those that survive are developmentally delayed [18,20]. Mutations in the *Fras1* gene produce epidermal-dermal adhesion defects which manifests as large blisters [19]. This is caused by a defective ECM arising from a mid-gestational developmental defect potentially accompanied by a dysregulation of TGF- β signalling [18]. This is consistent with the significantly lower adhesion of affected LM fibroblasts. Moreover, affected fibroblast conditioned media decreased the adhesion of normal fibroblasts implicating a secreted factor, potentially FRAS1, in this facet of the LM phenotype.

The diverse ADAMTS metalloprotease family are structurally similar to the MMP and ADAM proteases; accordingly, they possess similar and overlapping functionality [22,33]. The increased relative expression of *ADAMTS8* in affected fibroblasts was reproduced at the protein level. Elevated levels of *ADAMTS8* in affected fibroblasts can help explain their enhanced motility as the greater ECM remodelling leads to a less dense matrix which would otherwise impede migration [11]. Upregulation of *ADAMTS4* and *ADAMTS5*, which belong to the proteoglycanase sub-group alongside *ADAMTS8*, are involved in the over-degradation of cartilage ECM in osteoarthritis [11]. An analogous process could occur in LM, with *ADAMTS8* upregulation being a factor in the observed tissue atrophy. In nasopharyngeal carcinoma cell lines expressing *ADAMTS8*, apoptosis was induced and this could potentially act synergistically with the above mechanism to contribute to the atrophy [22]. *ADAMTSs* are secreted and are capable of cleaving and activating growth factors that are embedded in the ECM such as TGF- β 1; a process shared by MMPs, including MMP-2, which are also secreted

[34,35]. In normal fibroblasts overexpressing ADAMTS8, α -SMA protein was induced which is consistent with an effect on TGF- β 1 signalling.

Overall, these data highlight the importance of the secretome in LM and normal secretome replacement or addition of normal cells in affected areas may be a relatively simple and viable treatment. An improved understanding of the function of the altered LM secretome will lead to viable targeted therapies capable of modulating TGF- β 1 signalling with more control so as to prevent fibrosis and atrophy.

ACKNOWLEDGEMENTS

Experiments were designed by RO, LW, SB, IB and JH; and performed by SB, IB and LW; histological samples were provided by NS and BW; p-SMAD3 staining was performed by AR, PC and GI. RO, IB and SB are funded by the Great Ormond Street Children's Charity. This research was supported by the NIHR Great Ormond Street Hospital Biomedical Research Centre. The views expressed are those of the author(s) and not necessarily those of the NHS, the NIHR or the Department of Health.

REFERENCES

- [1] N. Fett, V.P. Werth, Update on morphea: Part I. Epidemiology, clinical presentation, and pathogenesis, *J. Am. Acad. Dermatol.* 64 (2011) 217–228. doi:10.1016/j.jaad.2010.05.045.
- [2] L. Weibel, J.I. Harper, Linear morphoea follows Blaschko's lines, *Br. J. Dermatol.* 159 (2008) 175–181. doi:10.1111/j.1365-2133.2008.08647.x.
- [3] A. Milano, S.A. Pendergrass, J.L. Sargent, L.K. George, T.H. McCalmont, M.K. Connolly, M.L. Whitfield, Molecular subsets in the gene expression signatures of scleroderma skin, *PLoS One.* 3 (2008). doi:10.1371/journal.pone.0002696.
- [4] J.J. Tomasek, G. Gabbiani, B. Hinz, C. Chaponnier, R.A. Brown, Myofibroblasts and mechano-regulation of connective tissue remodelling, *Nat. Rev. Mol. Cell Biol.* 3 (2002) 349–363. doi:10.1038/nrm809.
- [5] P. ten Dijke, C.S. Hill, New insights into TGF-beta-Smad signalling., *Trends Biochem. Sci.* 29 (2004) 265–73. doi:10.1016/j.tibs.2004.03.008.
- [6] N. Khalil, TGF-beta: from latent to active., *Microbes Infect.* 1 (1999) 1255–63. <http://www.ncbi.nlm.nih.gov/pubmed/10611753> (accessed May 15, 2012).
- [7] F. Huang, Y.-G. Chen, Regulation of TGF- β receptor activity., *Cell Biosci.* 2 (2012) 9. doi:10.1186/2045-3701-2-9.
- [8] P. Ngo, P. Ramalingam, J.A. Phillips, G.T. Furuta, Collagen gel contraction assay., *Methods Mol. Biol.* 341 (2006) 103–9. doi:10.1385/1-59745-113-4:103.
- [9] S. Su, S. Su, J. Chen, Collagen Gel Contraction Assay, *Protoc. Exch.* (2015). doi:10.1038/protex.2015.082.
- [10] A. Desmoulière, A. Geinoz, F. Gabbiani, G. Gabbiani, Transforming growth factor-beta 1 induces alpha-smooth muscle actin expression in granulation tissue myofibroblasts and in quiescent and growing cultured fibroblasts., *J. Cell Biol.* 122 (1993) 103–11. doi:10.1083/jcb.122.1.103.
- [11] C. Bonnans, J. Chou, Z. Werb, Remodelling the extracellular matrix in development and disease, *Nat. Rev. Mol. Cell Biol.* 15 (2014) 786–801. doi:10.1038/nrm3904.
- [12] E.W. Howard, B.J. Crider, D.L. Updike, E.C. Bullen, E.E. Parks, C.J. Haaksma, D.M. Sherry, J.J. Tomasek, MMP-2 expression by fibroblasts is suppressed by the myofibroblast phenotype, *Exp. Cell Res.* 318 (2012) 1542–1553. doi:10.1016/j.yexcr.2012.03.007.
- [13] J.F. Restrepo, R. Guzman, G. Rodriguez, A. Iglesias, Expression of transforming growth factor-beta and platelet-derived growth factor in linear scleroderma., *Biomedica.* 23 (2003) 408–415.
- [14] A.C. Daly, R.A. Randall, C.S. Hill, Transforming Growth Factor -Induced Smad1/5 Phosphorylation in Epithelial Cells Is Mediated by Novel Receptor Complexes and Is Essential for Anchorage-Independent Growth, *Mol. Cell. Biol.* 28 (2008) 6889–6902.

doi:10.1128/MCB.01192-08.

- [15] R.F.L. O'Shaughnessy, W. Yeo, J. Gautier, C.A.B. Jahoda, A.M. Christiano, The WNT signalling modulator, wise, is expressed in an interaction- dependent manner during hair-follicle cycling, *J. Invest. Dermatol.* 123 (2004) 613–621. doi:10.1111/j.0022-202X.2004.23410.x.
- [16] K.B. Lintern, S. Guidato, A. Rowe, J.W. Saldanha, N. Itasaki, Characterization of wise protein and its molecular mechanism to interact with both Wnt and BMP signals, *J. Biol. Chem.* 284 (2009) 23159–23168. doi:10.1074/jbc.M109.025478.
- [17] M. Yanagita, Inhibitors/antagonists of TGF- β system in kidney fibrosis., *Nephrol. Dial. Transplant.* 27 (2012) 3686–91. doi:10.1093/ndt/gfs381.
- [18] L. McGregor, V. Makela, S.M. Darling, S. Vrontou, G. Chalepakis, C. Roberts, N. Smart, P. Rutland, N. Prescott, J. Hopkins, E. Bentley, A. Shaw, E. Roberts, R. Mueller, S. Jadeja, N. Philip, J. Nelson, C. Francannet, A. Perez-Aytes, A. Megarbane, B. Kerr, B. Wainwright, A.S. Woolf, R.M. Winter, P.J. Scambler, Fraser syndrome and mouse blebbed phenotype caused by mutations in FRAS1/Fras1 encoding a putative extracellular matrix protein, *Nat. Genet.* 34 (2003) 203–208. doi:10.1038/ng1142.
- [19] K. Short, F. Wiradjaja, I. Smyth, Let's stick together: The role of the Fras1 and Frem proteins in epidermal adhesion, *IUBMB Life.* 59 (2007) 427–435. doi:10.1080/15216540701510581.
- [20] Q. Zhan, R.F. Huang, X.H. Liang, M.X. Ge, J.W. Jiang, H. Lin, X.L. Zhou, FRAS1 knockdown reduces A549 cells migration and invasion through downregulation of FAK signaling, *Int. J. Clin. Exp. Med.* 7 (2014) 1692–1697.
- [21] S.S. Apte, A disintegrin-like and metalloprotease (reprolysin-type) with thrombospondin type 1 motif (ADAMTS) superfamily: Functions and mechanisms, *J. Biol. Chem.* 284 (2009) 31493–31497. doi:10.1074/jbc.R109.052340.
- [22] G.C.G. Choi, J. Li, Y. Wang, L. Li, L. Zhong, B. Ma, X. Su, J. Ying, T. Xiang, S.Y. Rha, J. Yu, J.J.Y. Sung, S.W. Tsao, A.T.C. Chan, Q. Tao, The metalloprotease ADAMTS8 displays antitumor properties through antagonizing EGFR-MEK-ERK signaling and is silenced in carcinomas by CpG methylation., *Mol. Cancer Res.* 12 (2014) 228–38. doi:10.1158/1541-7786.MCR-13-0195.
- [23] A. Leask, D.J. Abraham, TGF-beta signaling and the fibrotic response., *FASEB J.* 18 (2004) 816–27. doi:10.1096/fj.03-1273rev.
- [24] T.J. Shaw, P. Martin, Wound repair: a showcase for cell plasticity and migration., *Curr. Opin. Cell Biol.* 42 (2016) 29–37. doi:10.1016/j.ceb.2016.04.001.
- [25] Y. Uziel, B.R. Krafchik, E.D. Silverman, P.S. Thorner, R.M. Laxer, Localized scleroderma in childhood: a report of 30 cases., *Semin. Arthritis Rheum.* 23 (1994) 328–40. doi:10.1016/0049-0172(94)90028-0.
- [26] L. Chung, J. Lin, D.E. Furst, D. Fiorentino, Systemic and localized scleroderma, *Clin. Dermatol.* 24 (2006) 374–392. doi:10.1016/j.clindermatol.2006.07.004.

- [27] A. Dańczak-Pazdrowska, M.J. Kowalczyk, B. Szramka-Pawlak, J. Gornowicz-Porowska, A. Szewczyk, W. Silny, M. Molińska-Glura, A. Olewicz-Gawlik, R. Zaba, J. Pazdrowski, P. Hrycaj, Transforming growth factor- β 1 in plaque morphea, *Postep. Dermatologii I Alergol.* 30 (2013) 337–342. doi:10.5114/pdia.2013.39431.
- [28] Y. Asano, H. Ihn, M. Jinnin, Y. Mimura, K. Tamaki, Involvement of α v β 5 integrin in the establishment of autocrine TGF- β signaling in dermal fibroblasts derived from localized scleroderma., *J. Invest. Dermatol.* 126 (2006) 1761–9. doi:10.1038/sj.jid.5700331.
- [29] R.A. Evans, Y.C. Tian, R. Steadman, A.O. Phillips, TGF- β 1-mediated fibroblast-myofibroblast terminal differentiation-the role of Smad proteins., *Exp. Cell Res.* 282 (2003) 90–100. <http://www.ncbi.nlm.nih.gov/pubmed/12531695>.
- [30] S. Petridou, O. Maltseva, S. Spanakis, S.K. Masur, TGF- β receptor expression and smad2 localization are cell density dependent in fibroblasts., *Invest. Ophthalmol. Vis. Sci.* 41 (2000) 89–95. <http://www.ncbi.nlm.nih.gov/pubmed/10634606>.
- [31] N. Itasaki, C.M. Jones, S. Mercurio, A. Rowe, P.M. Domingos, J.C. Smith, R. Krumlauf, Wise, a context-dependent activator and inhibitor of Wnt signalling., *Development.* 130 (2003) 4295–305. doi:10.1242/dev.00674.
- [32] A. Akhmetshina, K. Palumbo, C. Dees, C. Bergmann, P. Venalis, P. Zerr, A. Horn, T. Kireva, C. Beyer, J. Zwerina, H. Schneider, A. Sadowski, M.-O. Riener, O.A. MacDougald, O. Distler, G. Schett, J.H.W. Distler, Activation of canonical Wnt signalling is required for TGF- β -mediated fibrosis., *Nat. Commun.* 3 (2012) 735. doi:10.1038/ncomms1734.
- [33] R. Kelwick, I. Desanlis, G.N. Wheeler, D.R. Edwards, The ADAMTS (A Disintegrin and Metalloproteinase with Thrombospondin motifs) family, *Genome Biol.* 16 (2015) 113. doi:10.1186/s13059-015-0676-3.
- [34] N. Rocks, G. Paulissen, M. El Hour, F. Quesada, C. Crahay, M. Gueders, J.M. Foidart, A. Noel, D. Cataldo, Emerging roles of ADAM and ADAMTS metalloproteinases in cancer., *Biochimie.* 90 (2008) 369–79. doi:10.1016/j.biochi.2007.08.008.
- [35] T. Shiomi, V. Lemaître, J. D’Armiento, Y. Okada, Matrix metalloproteinases, a disintegrin and metalloproteinases, and a disintegrin and metalloproteinases with thrombospondin motifs in non-neoplastic diseases: Review Article, *Pathol. Int.* 60 (2010) 477–496. doi:10.1111/j.1440-1827.2010.02547.x.

Figure 1. LM affected fibroblasts are hyperproliferative, hypermigratory, with elevated collagen processing.

A. Histology of LM affected lesion and site-matched normal skin stained with haematoxylin and eosin; deep dermis denotes the reticular dermis distal from the epidermis. Bar 50 μm . **B.** Growth curve obtained from cell counts of primary human dermal fibroblasts isolated from LM affected lesions and site-matched normal skin cultured *in vitro* for 10 days. **C.** BrdU incorporation measured by absorbance (450 nm) in confluent normal and affected fibroblasts. **D.** Representative cell motility (scratch) assay image of normal and affected fibroblasts where the monolayer was scratched following a 30 min pre-incubation with mitomycin C (10 $\mu\text{g}/\text{ml}$) to inhibit proliferation, and the denuded area measured after 24 h in the continued presence of mitomycin C. Bar 50 μm . Graph (right) shows denuded area normalised to denuded area at 0 h. **E.** Collagen gel contraction assay performed on normal and affected LM fibroblasts for 8 days. Graph (right) shows gel area normalised to gel area at day 0. **F.** TGF- β 1 ELISA of conditioned media supernatant from overnight serum-starved normal and affected fibroblasts harvested after 24 h incubation. **G.** Representative western blot analysis (top) and zymography (bottom) of MMP-2 protein in lysates and conditioned media from normal and affected LM fibroblasts respectively. **H.** Graph of normalised MMP-2 activity in normal and affected conditioned media as measured by zymography. *** $P < 0.001$, ** $P < 0.01$, * $P < 0.05$, Paired T-test. All data expressed as mean \pm S.E.M. n=2 different normal and affected pairs. Representative data is shown.

Figure 2. LM affected fibroblasts are insensitive to exogenous TGF- β 1 and scratch wounding.

A. BrdU incorporation in confluent normal and affected fibroblasts treated with TGF- β 1 (12.5 ng/ml) or the control vehicle DMSO (0.1% v/v) for 24 h. **B.** Cell motility (scratch) assay of normal and affected fibroblasts after 24 h incubation with or without media conditioned for 24 h from the opposite fibroblast type in the presence of mitomycin C (10 $\mu\text{g}/\text{ml}$) with a 30 min pre-incubation. Graph (right) shows mean denuded area normalised to denuded area at 0 h. **C.** Cell adhesion assay of normal and affected fibroblasts incubated for 24 h with media alone, or TGF- β 1 (12.5 ng/ml), or media conditioned for 24 h with the opposite fibroblast type. Nucleic acid fluorescence is proportional to adherent cell number. * $P < 0.05$ vs normal, *** $P < 0.001$ vs normal, †† $P < 0.01$ vs normal + TGF- β 1, paired T-test. **D.** Representative immunofluorescence staining of SMAD2 in normal and affected fibroblasts *in vitro* 30 min post-scratch. **E.** Representative western blot of α -SMA (ACTA2) protein in normal and affected fibroblasts treated with or without TGF- β 1 (12.5 ng/ml) for 24 h. GAPDH was used as a loading control. **F.** Representative immunofluorescence staining of α -SMA (ASMA) protein in normal and affected fibroblasts *in vitro* 24 h post-scratch. Bar 50 μm . **G.** Representative western blot analysis of p-SMAD2 and p-SMAD3 protein in normal and affected fibroblasts treated with TGF- β 1 (12.5 ng/ml) for 30 min and 60 min. GAPDH was used as a loading control. Graphs (bottom) show normalised densitometry values. * $P < 0.05$ vs normal (0 min), † $P < 0.05$ vs affected (0 min), Paired T-test. All data expressed as mean \pm S.E.M. n=2 different normal and affected pairs. Representative data is shown.

Figure 3. Lack of SMAD2 phosphorylation is diagnostic of LM. **A.** Representative p and p-SMAD2 immunofluorescence and p-SMAD3 immunohistochemistry from the dermis of normal skin ($n = 5$), linear morphoea ($n = 9$), and scleroderma ($n = 3$). Bar 50 μm . **B.** Scoring of presence (black) or absence (white) of nuclear p-SMAD2 and p-SMAD3 in the dermis of normal skin (Nor), linear morphoea (Mor) or scleroderma (Scl). * $P < 0.05$, Fisher's exact test.

Figure 4. Gene expression analysis of differentially expressed genes in LM. **A.** Heat map and cluster analysis of significantly (> 2 fold, $P < 0.05$ in ≥ 4 of 5 sample pairs) differentially expressed genes (DEG) of matched normal and affected pairs ($n = 5$; 3 by microarray, 2 by RNAseq). Yellow denotes upregulation, blue downregulation. **B.** Gene ontology (GO) groups over-represented from the differentially expressed genes in LM fibroblasts. Results displayed as $1/P$ value with Bonferroni correction for multiple testing. **C.** Mean fold change of differentially expressed secreted factors in LM fibroblasts. **D.** Pairwise investigation (N1 vs A1, N2 vs A2, etc.) of *ADAMTS8*, *FRAS1* and *SOSTDC1* expression in 5 pairs of samples. P values are shown for Wilcoxon rank sum test.

Figure 5. Sostdc1 knockdown increases migration, reduces proliferation, and causes TGF- β 1 insensitivity. **A.** Representative immunofluorescence staining of SOSTDC1 in normal and affected LM skin tissue *ex vivo*. **B.** Representative western blot analysis of SOSTDC1 protein in cell lysate and conditioned media supernatant from normal and affected LM fibroblasts cultured *in vitro*. GAPDH was used as a loading control. **C.** Representative western blot analysis of Sostdc1 protein in conditioned media supernatant from mouse NIH 3T3 fibroblasts transfected with either a scrambled sequence shRNA control or Sostdc1 shRNA, and processed with or without PNGase. Equal loading of conditioned medium was confirmed with Ponceau red (B, C). **D.** Growth curve of scrambled shRNA or Sostdc1 shRNA transfected NIH 3T3 fibroblasts cultured for 10 days. * $P < 0.05$ vs scrambled shRNA (day 10). **E.** Cell motility (scratch) assay of scrambled shRNA or Sostdc1 shRNA transfected NIH 3T3 fibroblasts after 24 h in the presence of mitomycin C (10 $\mu\text{g}/\text{ml}$) with a 30 min pre-incubation. Graph (bottom) shows denuded area normalised to denuded area at 0 h. * $P < 0.05$ vs scrambled shRNA. **F.** NIH 3T3 fibroblasts transfected with either scrambled shRNA or Sostdc1 shRNA, in which lysates were subjected to gelatin zymography (top) or western blot analysis (bottom) of MMP-2. **G.** Representative western blot analysis of p-SMAD2 and SMAD2 protein in NIH 3T3 fibroblasts transfected with either scrambled shRNA or Sostdc1 shRNA, with or without TGF- β 1 treatment (12.5 ng/ml) for 3 or 6 h. GAPDH was used as a loading control. **H.** Representative western blot analysis of α -SMA (ACTA2) protein in NIH 3T3 fibroblasts transfected with either scrambled shRNA or Sostdc1 shRNA, and treated with or without TGF- β 1 (12.5 ng/ml) with increasing duration of serum starvation (0, 2 or 24 h). GAPDH was used as a loading control. All data expressed as mean \pm S.E.M. unpaired T-test, $n=3$ biological replicates. Representative data is shown

Figure 6. FRAS1 dermal expression is reduced in LM skin; ADAMTS8 overexpression induces smooth muscle actin expression. **A.** Representative western blot analysis of FRAS1 protein levels in normal and LM affected fibroblasts. GAPDH was used as a loading control. Graph (right) shows normalised FRAS1 intensity. **B.** Representative immunofluorescence staining of FRAS1 in skin tissue harvested from LM affected lesions (n=9) and normal skin (n=5). Graph (bottom) shows fluorescence normalised to cell number. * $P < 0.05$, unpaired T-Test. **C.** Representative western blot analysis of ADAMTS8 protein levels in normal and LM affected fibroblasts. Graph (right) shows normalised ADAMTS8 intensity. **D.** Representative immunofluorescence staining of ADAMTS8 in primary dermal fibroblasts from LM affected lesions and site-matched normal skin. **E.** Representative western blot analysis of α -SMA (ASMA) and ADAMTS8 in normal (N) or LM affected (n=3 biological replicates) (A) fibroblasts and normal fibroblasts transduced with either an empty vector control or an ADAMTS8 overexpression vector. GAPDH was used as a loading control. All data expressed as mean \pm S.E.M.

1 TABLES

Table 1. Clinical characteristics of patients with LM

Patient	Sex	Age (years)	Biopsy site
1	Female	10	Thigh
2	Female	12	Knee
3	Male	8	Lower leg
4	Male	17	Thigh
5	Female	10	Thigh

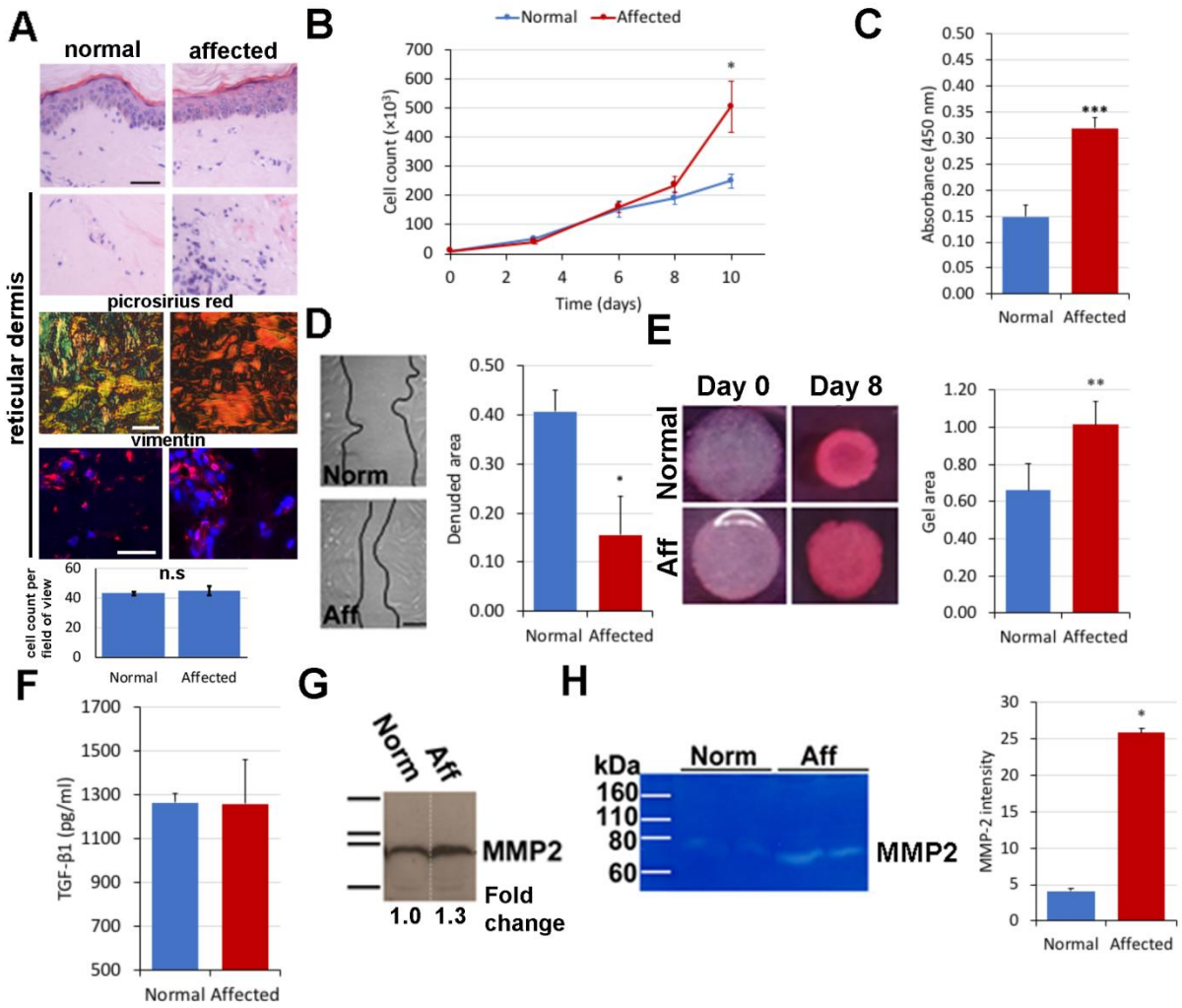
Clinical characteristics of patients with LM from whom biopsies were obtained. Primary dermal fibroblasts were isolated from affected (A) lesions and site-matched normal (N) regions. All patients were on methotrexate at time of harvest.

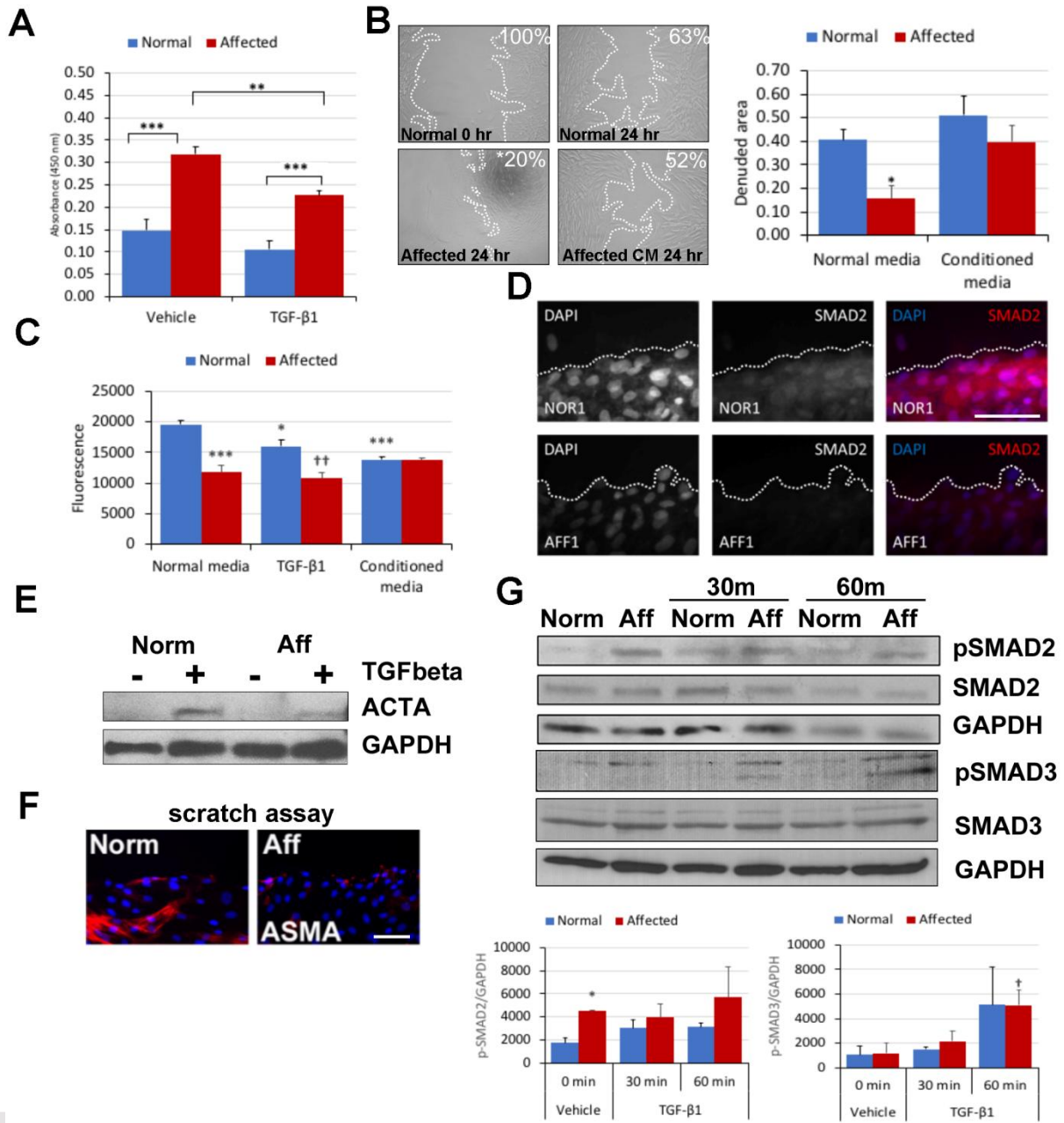
Table 2. Differentially expressed genes in LM

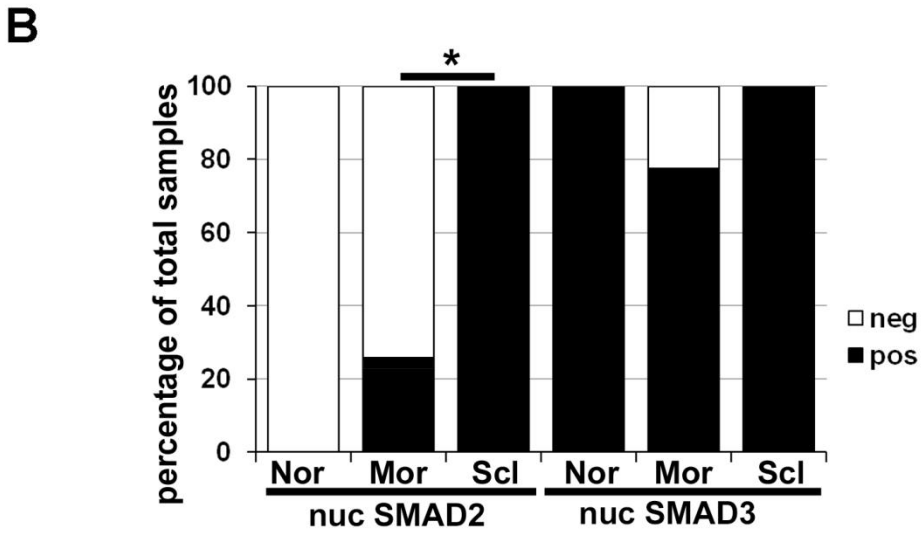
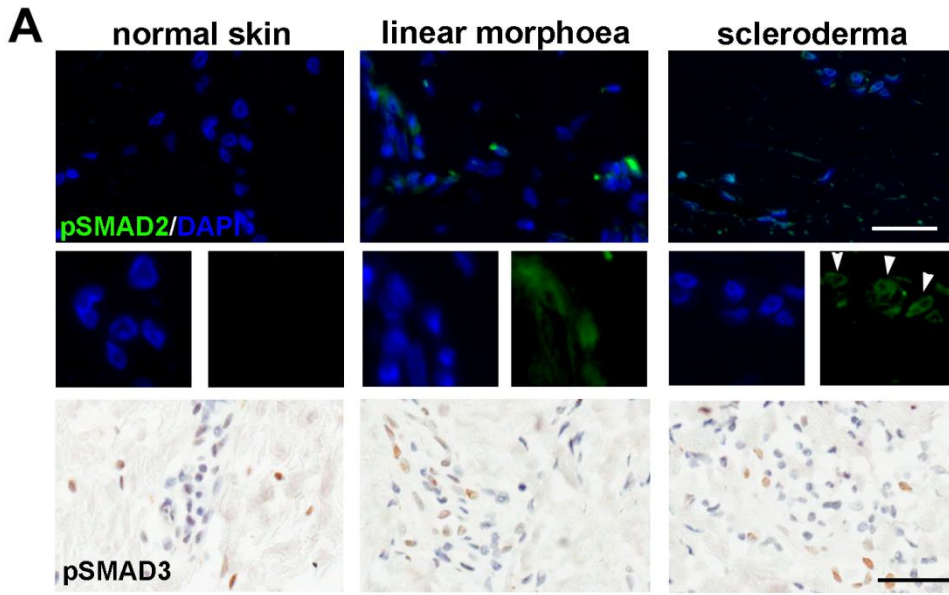
Gene	Affymetrix			RNA-Seq		Affymetrix			RNA-Seq		Relative to N		p value
	N1	N2	N3	N4	N5	A1	A2	A3	A4	A5	Log FC	FC	
ADAMTS8	-1.71	-2.46	-2.67	-1.66	-1.66	3.06	1.71	3.05	1.66	1.66	4.26	19.15	0.00
SLC14A1	-1.88	-1.64	-0.89	-1.66	-1.66	1.64	0.89	1.28	1.66	1.66	2.97	7.86	0.00
EVI2A	-0.93	-0.63	-1.51	NaN	-1.98	2.16	0.63	0.84	NaN	1.98	2.66	6.34	0.00
NOV	-2.11	-2.28	-1.00	-0.84	0.57	2.56	1.13	1.00	0.84	-0.57	2.12	4.35	0.02
CRIP1	-0.48	-1.92	-0.64	-0.79	NaN	0.48	0.59	1.08	0.79	NaN	1.69	3.23	0.01
CD74	-0.83	-0.39	-0.42	-1.69	0.67	1.17	0.39	1.90	1.69	-0.67	1.43	2.69	0.05
PPIL2	-0.50	-0.74	-0.64	NaN	-0.55	0.66	0.50	0.71	NaN	0.55	1.21	2.32	0.00
PPP1R13L	0.45	1.22	0.55	0.83	-0.54	-0.46	-0.56	-0.45	-0.83	0.54	-0.86	0.55	0.05
PPAPDC1A	1.34	0.63	0.53	1.19	-0.67	-1.17	-0.71	-0.53	-1.19	0.67	-1.19	0.44	0.04
EXPH5	0.38	1.37	0.67	0.96	-0.55	-0.38	-1.55	-1.73	-0.96	0.55	-1.38	0.38	0.03
IL18R1	0.29	-0.28	0.28	1.66	1.51	1.41	-1.68	-1.67	-1.66	-1.51	-1.71	0.30	0.05
KRT19	0.37	2.80	0.77	-0.70	1.58	-0.54	-2.47	-0.37	0.70	-1.58	-1.81	0.29	0.05
VWVC1	-0.16	1.83	0.16	0.90	1.66	0.82	-1.83	-1.22	-0.90	-1.66	-1.84	0.28	0.02
AMIGO2	1.32	1.88	0.52	0.93	NaN	-0.64	-1.00	-0.52	-0.93	NaN	-1.93	0.26	0.00
GRTP1	0.07	1.59	1.17	1.66	NaN	-0.07	-1.05	-0.47	-1.66	NaN	-1.93	0.26	0.01
LHX8	1.43	-1.00	1.10	1.66	1.66	0.82	-2.17	-0.82	-1.66	-1.66	-2.07	0.24	0.02
FRAS1	0.97	0.44	0.78	1.66	1.66	-0.89	-0.67	-0.44	-1.66	-1.66	-2.17	0.22	0.00
BBOX1	1.45	3.29	-0.04	0.84	NaN	0.04	-0.77	-2.03	-0.84	NaN	-2.28	0.21	0.04
MDFI	-0.02	1.17	0.02	1.66	NaN	0.08	-3.53	-1.48	-1.66	NaN	-2.35	0.20	0.04
COL22A1	0.78	3.67	0.25	NaN	0.87	-0.25	-1.08	-2.21	NaN	-0.87	-2.50	0.18	0.04
PI16	1.60	-1.57	1.06	2.31	2.48	1.26	-1.06	-2.20	-2.31	-2.48	-2.53	0.17	0.04
CCL11	-0.58	2.20	0.58	1.66	1.66	1.02	-3.12	-2.05	-1.66	-1.66	-2.60	0.17	0.02
F11R	0.98	4.25	-0.08	0.58	1.66	0.08	-1.89	-2.05	-0.58	-1.66	-2.70	0.15	0.02
TPD52	0.83	2.69	0.85	0.61	1.66	-0.83	-3.43	-2.46	-0.61	-1.66	-3.12	0.11	0.00
TMEM176B	0.84	3.66	0.77	0.72	NaN	-0.77	-3.73	-1.35	-0.72	NaN	-3.14	0.11	0.02
TRIM29	1.28	4.71	0.09	NaN	0.74	-0.09	-2.49	-2.52	NaN	-0.74	-3.16	0.11	0.05
CXADR	1.24	4.30	-0.04	0.98	NaN	0.04	-1.87	-3.57	-0.98	NaN	-3.21	0.11	0.04
LIPG	1.06	3.47	-0.58	1.11	1.35	0.58	-3.47	-4.73	-1.11	-1.35	-3.30	0.10	0.02
EFNA1	1.37	5.46	0.32	0.61	0.74	-0.32	-3.56	-2.83	-0.61	-0.74	-3.31	0.10	0.02
LAMC2	0.83	3.96	-0.18	NaN	0.91	0.18	-3.53	-3.48	NaN	-0.91	-3.32	0.10	0.04
F2RL1	0.06	3.91	-0.06	1.66	NaN	1.02	-3.88	-3.46	-1.66	NaN	-3.39	0.10	0.06
ANXA8	1.22	4.58	0.05	NaN	1.68	-0.05	-2.89	-2.08	NaN	-1.68	-3.56	0.08	0.03
SOSTDC1	1.57	4.64	0.52	-1.05	1.66	-0.52	-4.52	-4.93	1.05	-1.66	-3.58	0.08	0.04
TP63	1.30	5.15	0.46	NaN	1.66	-0.46	-1.73	-2.29	NaN	-1.66	-3.68	0.08	0.03
SFN	1.33	3.87	0.02	1.66	NaN	-0.02	-3.39	-3.06	-1.66	NaN	-3.76	0.07	0.01
C19orf33	2.17	4.96	0.40	1.66	NaN	-0.58	-0.40	-3.21	-1.66	NaN	-3.76	0.07	0.02
IL18	1.27	5.49	1.32	NaN	1.66	-1.27	-1.84	-2.25	NaN	-1.66	-4.19	0.05	0.02
KRT5	1.21	4.40	0.19	0.53	1.66	-0.19	-6.57	-7.22	-0.53	-1.66	-4.83	0.04	0.03
KRT6	1.05	5.43	0.13	NaN	1.58	-0.13	-7.92	-5.53	NaN	-1.58	-5.84	0.02	0.04

Gene expression analysis by Affymetrix (N1, N2, N3, A1, A2, A3) and RNA-Seq (N4, N5, A4, A5) of LM normal (N) and affected (A) fibroblasts. 39 genes were significantly differentially expressed in ≥ 4 of 5 sample pairs.

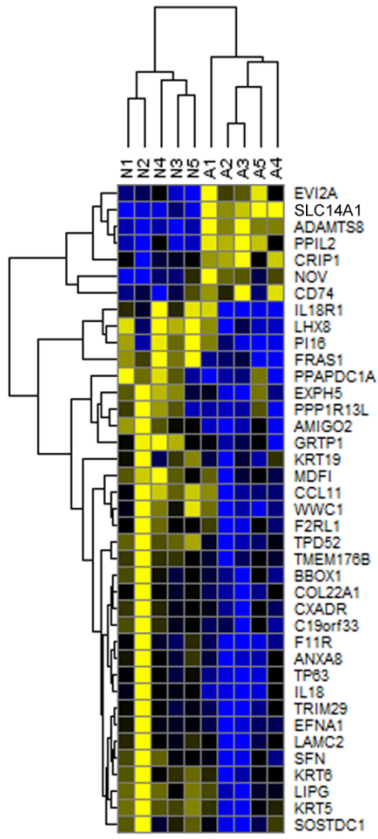
Data normalised and sorted by log fold change (FC). Yellow denotes upregulation, blue downregulation. NaN, not a number.



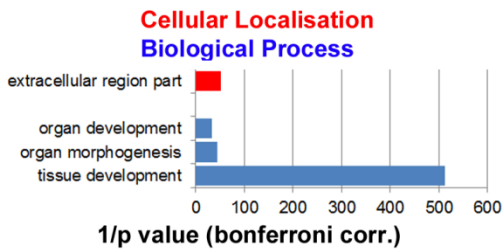




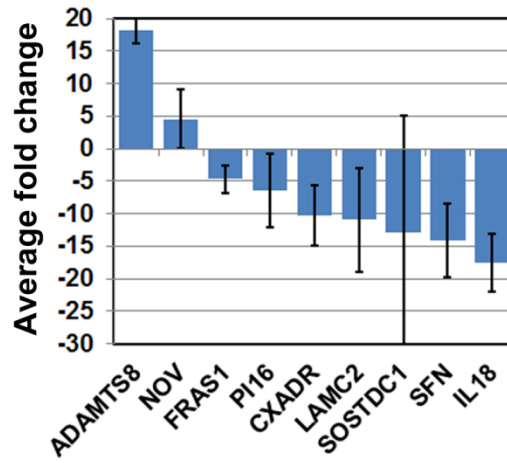
A



B



C



D

